A 2D FSI MODEL FOR PAPER WEBS AND FABRICS MOVING CLOSE TO EACH OTHER IN COMPLEX GEOMETRIES

By

Eero Immonen[1], Fredrik Bergström[1], Simo Nurmi[1], Antti Lehtinen[1], Kari Juppi[2], Lars Martinsson[3]
[1]Process Flow Ltd Oy
[2]Metso Paper Oy
FINLAND
[3]Albany International AB
SWEDEN

ABSTRACT

In the present article we develop a two-dimensional computational fluid-structure interaction (FSI) model for small transverse deflections of a moving paper web, supported on one side by a fabric, both moving in an arbitrary geometry containing boundaries and nips (e.g. as in the drying section of a paper machine). In our FSI model, the transverse deflections of the paper web and those of the fabric are *individually* assumed to satisfy an equation of motion for axially moving membranes, such as:

$$m\frac{\partial^2 w}{\partial t^2} + 2mv\frac{\partial^2 w}{\partial x \partial t} + (T - mv^2)\frac{\partial^2 w}{\partial x^2} = f(\Delta p, g, a, c) \qquad \{1\}$$

Displacements $w(x,t)$ in Equation {1} are induced by the pressure difference profile Δp across the membrane, gravity g, adhesion a, and centrifugal forces c, as well as any contacts with boundaries. The equations for the fabric and the web utilize different tension and mass parameters T_{fabric}, T_{paper}, m_{fabric}, m_{paper} but the axial velocities coincide, i.e. $v_{fabric} = v_{paper}$. The pressure differences across the web (Δp_{paper}) and fabric (Δp_{fabric}) are obtained by numerically solving the Navier-Stokes equations for air flow motion around the paper web and the fabric. This air flow motion results from the motion of solids in the flow field, and it also generates subsequent motion of solids through the coupling in Equation {1}. A remarkable feature of this FSI model is that it is to a large degree geometry-independent, and hence applicable in a wide array of paper machine regions. In particular, the model is suitable for such modern paper machine drying sections which are arranged in the modern *single-run* configuration, whereby the wet paper web is only supported by a dryer fabric on one of its sides. We show by qualitative examples that the proposed FSI model yields useful results in realistic single-run geometries. The inclusion of fabric dynamics in the model provides an important and non-trivial extension of a recent FSI model covering paper web dynamics only in the same context.

INTRODUCTION

Having reached the practical width limit for paper machines, the paper machine manufacturers worldwide are now focusing on achieving higher paper web speeds in order to meet ever-increasing productivity requirements. In fact, it is not uncommon for a production machine today to reach a web speed of 2000 meters per minute. Such high web velocities are facilitated, among other things, by the so-called *single-run configuration*, whereby the wet paper web is only supported on one of its sides by a dryer fabric throughout the paper machine's drying section. Achieving such high web velocities is not an easy task, however, as the resulting air flow effects cause severe runnability issues. In particular, the effects of millimeter-scale transverse web deflections that are often seen at the nip regions of a drying section are notoriously difficult to mitigate in practice, and yet their presence (or lack thereof) can have a tremendous impact on the maximum speed at which the paper machine can be run. Today, paper machines incorporate sophisticated equipment for the regulation of pressures at nip regions in order to control the onset of web deflections, but there is still a need to more thoroughly understand the mechanisms that induce these deflections. In particular, it has been observed in practice that in a single-run system, the dryer fabric microstructure can have a significant effect on overall runnability. However, at present there appears to be no theory to explain this effect. In this article, we attempt to enhance the understanding of web and fabric kinematics in paper machines through FSI modeling.

The study of paper web dynamics has been fairly active during the past decades; the reader is referred to Chang and Moretti (1991), Koivurova (1998), Müftü and Cole (1999), Kurki (2005) and Immonen et al. (2009). Reference [5] also provides an up-to-date literature review on the topic. Recently, Immonen et al. (2009) introduced a computational 2D FSI model for small transverse deflections of high-velocity paper webs for the paper making environment. They concluded that their model could reproduce the aforementioned web pocketing phenomena in realistic single-run geometries. However, their model assumes that the fabric (if it exists in the geometry) is not subject to deformations. Now, a dryer fabric in a single-run system – although relatively stiff in practice – is never fully rigid. Consequently, its motion is coupled to that of the paper web. In this light it is evident that the model of Immonen et al. (2009) is not accurate at such regions where the paper web would move the dryer fabric due to a pressure gradient across the web-fabric combination. In practice, this occurs throughout the drying sections of high-speed single-run systems. The main purpose of this article is to extend the model FSI model of Immonen et al. (2009) to take into account fabric dynamics and thus improve the overall model accuracy.

While models of paper web dynamics have been published in the academic literature, to the authors' knowledge relatively little is known about the modeling of fabric dynamics in a paper machine. Further, there are some significant challenges related to the modeling of *joint* dynamics of paper webs and dryer fabrics in this context:

- Although the wet paper web can be reasonably considered infinitely thin in FSI simulations, the dryer fabric does have a positive (albeit small) thickness. This makes contact treatment for web and fabric rather elaborate in the more complex actual paper machine geometries.
- The wet paper web has been observed to be virtually impermeable in practice, whereas the dryer fabric is always permeable to a degree. Accurate modeling of 3D fabric microstructure in 2D is thus necessary in order to obtain realistic FSI models for industrial applications.

- In practice, the mass and tension of a dryer fabric are often an order of magnitude larger than those of the paper web. Consequently, the web dynamics may be relatively unstable compared to fabric dynamics, which may cause difficulties in the numerical solution of the problem.
- Fabric motion can induce web motion and web motion can induce fabric motion in different contact situations. This lack of fixed input-output structure imposes considerable flexibility requirements for the FSI model.

Our approach for modeling web dynamics is the same as in Immonen et al. (2009), whereas the fabric kinematics is based on the assumptions of Euler-Bernoulli beam theory. In the applications we have in mind, the fabric length is much larger than its thickness, the fabric cross section is roughly constant along its axis, the fabric is loaded in its plane of symmetry, all fabric deformations remain small, and, plane sections of the fabric remain roughly planar under deformations. A key observation that one can make under these assumptions is the following: the dynamics of both the (infinitely thin) paper web and the fabric (of positive thickness) can be described by appropriately modifying the PDE (1). This is the essence of the 2D FSI model for paper webs and fabrics proposed in the present article. Our approach consists of:

i. Numerically solving a PDE system based on Equation {1} for the transverse deflections $w_f(x,t)$ of the *fabric-to-paper* surface;
ii. Applying the deflections $w_f(x,t)$ rigidly to the opposite *fabric-to-air* surface as in the Euler-Bernoulli framework;
iii. Numerically solving a PDE system based on Equation {1} for the transverse deflections $w(x,t)$ of the *paper web*;
iv. Numerically solving the Navier-Stokes equations for the air flow surrounding the paper web and the fabric;
v. Keeping track of possible contact situations and adjusting the aforementioned solutions w_f and w accordingly.

Fluid-structure interaction takes place in the proposed model as follows: The motion of solid structures (including the paper web and the fabric) causes movement of the surrounding air, which results in a nonzero pressure difference profiles Δp and Δp_f across the paper web and the fabric. These pressure difference profiles induce deflections to the web and the fabric, which in turn cause changes in the surrounding air flow field, thus concluding the FSI cycle. While the displacement model for the fabric does not take into account fabric microstructure, its CFD model does take it into account. Furthermore, in our FSI model, fabric motion can induce web motion and vice versa through inelastic collisions. The proposed FSI model has been implemented in a commercial CFD solver, ANSYS Fluent, the FEM part of it being a proprietary DLL extension that applies the Hilber-Hughes-Taylor method to a Galerkin-discretized system of ordinary differential equations.

The benefits and drawbacks of the proposed approach are by and large the same as those in ref. [5]. Being virtually independent of the 2D geometry, the model is particularly suitable for describing large portions of drying sections in single-run configured paper machines; in such applications the web and fabric deflections are *a priori* known to be small. However, web and fabric treatment being purely transverse and linear, the models presented in this paper cannot be used for predicting large deflections from the initial state, nor general transverse deflections of a curvilinear (unsupported) web, nor the axial deflections of the paper web. In addition to this, in our model, the web and fabric are assumed to be uniform with constant tensions, masses and axial velocities. These assumptions are clearly restrictive in some applications.

NOMENCLATURE

Notation	Description	Units
$w(x,t)$, $w_f(x,t)$	Transverse displacement at point x and time t	m
v	Axial web velocity	m/s
T, T_f	Tension	N/m
m, m_f	Mass per unit area	kg/m^2
$\Delta p, \Delta p_f$	Pressure difference	Pa
x	Spatial coordinate along the web	m
t	Time	s
$\Omega_f(t), \Omega_p(t)$	Set of points in contact with boundary $\mathcal{B}$	-
$\Omega_{fp}(t)$	Set of web points in contact with fabric	-
$\mathcal{F}, \mathcal{F}_a, \mathcal{F}_p$	Set of initial locations of fabric and its surfaces (fabric-air, fabric-paper)	-
$\wp$	Set of initial locations of paper web points	-
$\mathcal{G}$	The overall plane geometry	-
$\mathcal{B}$	Set of points in boundaries	-
$\varkappa, \varkappa_{fp}, \varkappa_f$	Contact functions	-
$\varkappa'$	Contact change function for the web	-
L	Length of web and fabric	m
$\boldsymbol{R}(x), \boldsymbol{R}_f(x)$	Signed local radius of curvature at point x	m/s
$\boldsymbol{g}$	Gravitational acceleration vector	m/s^2
W	Adhesion energy	J/m^2
$\mathcal{L}$	Parameterization by curve length (function)	-
ϕ	Opening/closing angle of web contact	-
$dist(A,B)$	Minimum distance between sets A and B	-
ϵ_f, ϵ_p	Minimum allowed distance to a boundary	m
ϵ_{defl}	Maximum deflection	m
ϵ_{fp}	Minimum allowed distance between web and fabric	m
C	Coefficient in the fabric CFD model	kg/m^4
D	Coefficient in the fabric CFD model	kg/ m^{3}s

THE FSI MODEL

Mathematical Model for Web and Fabric Dynamics

Our kinematic deflection model is based on the assumption that the deforming medium (i.e. web or fabric) is moving *locally axially* at a constant velocity, while it can undergo time-dependent *transverse displacements* with respect to its initial state (profile). By local axial motion we mean that the local tangential motion of the medium is close to being collinear with its primary axis, and by transverse displacements we refer to deflections that are locally orthogonal to the initial state; see the figure below.

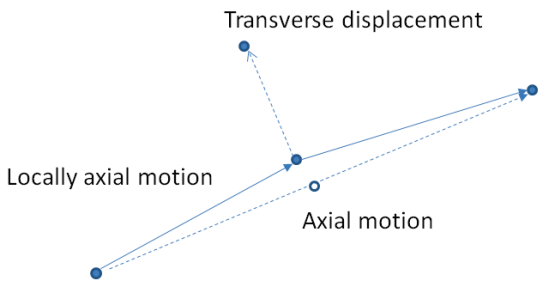

Figure 1 – Axial motion, locally axial motion and transverse displacement

The mathematical web and fabric deflection model, presented below, is built on the following concepts (all sets below are, of course, nonempty):

- A given *geometry* $\mathcal{G}$, which is a closed and bounded set of the plane $\mathbb{R}^2$.
- A given subset $\mathcal{P} \subset \mathcal{G}$, which we call the *paper web*, for which there exists a finite length L and an injective and continuously differentiable length parameterization function $\mathcal{L} : \mathbb{R} \to \mathbb{R}^2$ such that $\mathcal{L}([0, L]) = \mathcal{P}$.
- A given subset $\mathcal{B} \subset \mathcal{G} \setminus \mathcal{P}$ which we call the (non-deforming) *boundary*.
- A given subset $\mathrm{F} \subset \mathcal{G} \setminus (\mathcal{P} \cup \mathcal{B})$, which we call the *fabric*, with two distinct topological boundaries $\mathrm{F_p}$ (*fabric-paper surface*) and $\mathrm{F_a}$ (*fabric-air surface*) such that:
  - There exists injective and continuously differentiable length parameterization functions $\mathcal{L}_{fp} : \mathbb{R} \to \mathbb{R}^2$ and $\mathcal{L}_{fa} : \mathbb{R} \to \mathbb{R}^2$ such that $\mathcal{L}_{fp}([0, L]) = \mathrm{F_p}$ and $\mathcal{L}_{fa}([0, L]) = \mathrm{F_a}$,
  - The fabric thickness is uniform, i.e. $dist\,(\mathcal{L}_{fa}(x), \mathcal{L}_{fp}(x)) = d_{fabric} > 0$ for all $x \in [0, L]$.
  - The initial web-fabric distance is uniform, i.e. $dist\,(\mathcal{L}(x), \mathcal{L}_{fp}(x)) = d_{fp} > 0$ for all $x \in [0, L]$.
  - The fabric surfaces are arranged such that $dist\,(\mathcal{L}(x), \mathcal{L}_{fa}(x)) = d_{fp} + d_{fabric}$ for all $x \in [0, L]$.
- A *fabric-boundary contact function* $\varkappa_f : [0, L] \times \mathbb{R} \to \{0,1\}$ whose arguments are the length x along the fabric and the corresponding fabric deflection $w_f(x, \cdot)$ (but not time). The function $\varkappa_f$ is constructed based on $\mathcal{B}$, the minimum allowable fabric-boundary distance $\epsilon_f > 0$, and fabric thickness d_{fabric}. It uniquely determines the set $\Omega_f(t_0)$ of fabric points in contact with a boundary point for each $t_0 > 0$:
$$\Omega_f(t_0) = \left\{ x \in [0, L] \;\middle|\; \varkappa_f\left(x, w_f(x, t_0)\right) = 1 \right\}$$
- A *web-fabric contact function* $\varkappa_{pf} : [0, L] \times \mathbb{R} \times \mathbb{R} \to \{0,1\}$ whose arguments are the length x along the web *and* fabric, the corresponding web deflection $w(x, t)$ and the corresponding fabric deflection $w_f(x, t)$ (but not time). The function $\varkappa_{pf}$ is constructed based on minimum allowable fabric-

paper distance $\epsilon_{fp} > 0$ and it uniquely determines the set $\Omega_{pf}(t_0)$ of points where the web and fabric are in contact at a given instant $t_0 > 0$ of time:

$$\Omega_{pf}(t_0) = \{ x \in [0, L] \mid \varkappa_{pf}(x, w_f(x, t_0), w(x, t_0)) = 1 \}$$

- A *web-boundary contact function* $\varkappa : [0, L] \times \mathbb{R} \to \{0,1\}$ whose arguments are the length x along the web and the corresponding web deflection $w(x,\cdot)$ (but not time). The function $\varkappa$ is constructed based on $\mathcal{B}$ and the minimum allowable web-boundary distance $\epsilon_p > 0$. It uniquely determines the set $\Omega_p(t_0)$ of web points in contact with a boundary point at each instant $t_0 > 0$ of time:

$$\Omega_p(t_0) = \{ x \in [0, L] \mid \varkappa(x, w(x, t_0)) = 1 \}$$

- The (formal) derivative function $\varkappa' : (0, L) \times \mathbb{R} \to \{0,1\}$ which describes *web attachment* and *web detachment from* $\mathcal{B}$ (change of contact status) through the conventions:
  - $\varkappa'(x_0, w(x_0,\cdot)) = 1$ if $\varkappa(x_0, w(x_0,\cdot)) = 1$ and $\varkappa(x, w(x,\cdot)) = 0$ for all $x \in (x_0, x_0 + \delta]$ and some $\delta > 0$ (opening contact in the web's indexing direction)
  - $\varkappa'(x_0, w(x_0,\cdot)) = 1$ if $\varkappa(x_0, w(x_0,\cdot)) = 1$ and $\varkappa(w(x,\cdot)) = 0$ for all $x \in [x_0 - \delta, x_0)$ and some $\delta > 0$ (closing contact in the web's indexing direction).
  - $\varkappa'(x, w(x,\cdot)) = 0$ otherwise.

As an extension to the model of Immonen, et al. (2009), we propose the following kinematic model for the *fabric*:

$$m_f \frac{\partial^2 w_f(x,t)}{\partial t^2} + 2 m_f v \frac{\partial^2 w_f(x,t)}{\partial x \partial t} + \left(T_f - m_f v^2\right) \frac{\partial^2 w_f(x,t)}{\partial x^2} = F_1(x,t) \quad \{2a\}$$
$$t > 0, x \notin \Omega_{pf}(t)$$

$$m_f \frac{\partial^2 w_f(x,t)}{\partial t^2} + 2 m_f v \frac{\partial^2 w_f(x,t)}{\partial x \partial t} + \left(T_f - m_f v^2\right) \frac{\partial^2 w_f(x,t)}{\partial x^2} = F_2(x,t), t > 0, x \quad \{2b\}$$
$$\in \Omega_{pf}(t) / \Omega_f(t)$$

$$\frac{\partial^2 w_f(x,t)}{\partial t^2} = \frac{\partial w_f(x,t)}{\partial t} = 0, t > 0, x \in \Omega_f(t) \quad \{2c\}$$

$$w_f(0,t) = w_f(L,t) = 0 \quad \forall t, \quad w_f(x,0) = 0 \quad \forall x \in [0, L] \quad \{2d\}$$

under the assumption that $T_f - m_f v^2 > 0$. By convention, $w_f(x,t) > 0$ indicates fabric displacement towards the web. Equation {2a} describes the no-contact dynamics of the fabric. In Equation {2a} the driving term $F_1(x,t)$ equals the sum of:

- pressure difference across the fabric, $\Delta p_f(x,t)$, calculated from the surrounding air flow;

- gravity contribution $g_f(x) = m_f \boldsymbol{g} \cdot \boldsymbol{n^0}(x)$, where $\boldsymbol{n^0}(x)$ is the local unit normal vector for the fabric;
- local centrifugal force contribution $c_f(x) = \frac{T_f - m_f v^2}{\boldsymbol{R}_f(x)}$, where $\boldsymbol{R}_f(x)$ is the signed local radius of curvature[1] at fabric point $x \in [0, L]$.

On the other hand, Equation {2b} describes the dynamics of those fabric points which are in contact with the paper web but not with boundary $\mathcal{B}$. The only difference to Equation {2a} is in the driving term is $F_2(x,t)$; it is the same as $F_1(x,t)$ except for the pressure difference term, which in Equation {2b} is now $\Delta p_f(x,t) + \Delta p(x,t)$. Finally, Equation {2c} describes freezing of fabric regions in contact with $\mathcal{B}$, and Equation {2d} provides the initial and boundary conditions.

As an extension to the model of Immonen et al. (2009), we propose the following kinematic model for the *web*:

$$m\frac{\partial^2 w(x,t)}{\partial t^2} + 2mv\frac{\partial^2 w(x,t)}{\partial x \partial t} + \left(T - mv^2\right)\frac{\partial^2 w(x,t)}{\partial x^2} = F(x,t), \quad t > 0,\ x \notin \Omega_p(t) \cup \Omega_{pf}(t) \quad \{3a\}$$

$$w(x,t) - w_f(x,t) = \epsilon_{fp}, \quad t > 0, x \in \Omega_{pf}(t) \setminus \Omega_p(t) \quad \{3b\}$$

$$\frac{\partial^2 w(x,t)}{\partial t^2} = \frac{\partial w(x,t)}{\partial t} = 0, \quad t > 0, x \in \Omega_p(t) \quad \{3c\}$$

$$w(0,t) = w(L,t) = 0 \quad \forall t, \quad w(x,0) = 0 \quad \forall x \in [0, L] \quad \{3d\}$$

under the assumption that $T - mv^2 > 0$. By convention, $w(x,t) > 0$ indicates web displacement away from the fabric. The interpretation of Equation {3} is analogous to that of Equation {2}. However, in Equation {3a} the driving term $F(x,t)$ also includes as a summand the normal local adhesion $\|\boldsymbol{a}(x,t)\| = N_{adh}(x,t) = \frac{W \sin\phi}{\cos\phi}\varkappa'(w(x,t))$ that is being applied to such web nodes where contact status with respect to the non-deforming boundary $\mathcal{B}$ is changing. Also note that Equation {3b} describing web-fabric contact requires knowledge of the fabric displacement profile $w_f(x,t)$. In other words, the larger momentum of the fabric determines the joint motion of such web and fabric points which are in contact with each other.

The figures below illustrate the above source term contributions to Equations {2a} and {3a}.

---

[1] Note that in numerical simulations, the function $\boldsymbol{R}_f(x)$ can be algorithmically constructed based on knowledge of the geometry and the direction of web motion alone. Indeed, one can consider sets of three consequtive web points x_{i-1}, x_i, x_{i+1} (as in Figure) and set $\boldsymbol{R}_f(x_i) = \infty$ if the three points are collinear and otherwise set $\boldsymbol{R}_f(x_i) = r$, where r is the radius of circumcircle through x_{i-1}, x_i, x_{i+1} as in ref. [11]. The sign of $\boldsymbol{R}_f(x_i)$ can then be deduced from direction of web motion and the (freely assignable) positive direction for web displacements.

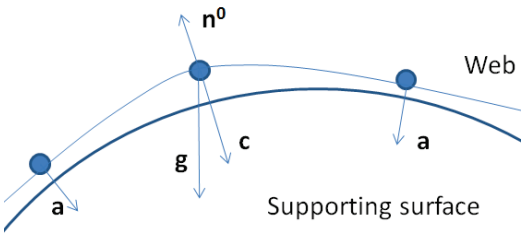

Figure 2 – Adhesion forces (a), gravity (g), centrifugal force (c) and local unit normal vector $\boldsymbol{n^0}$

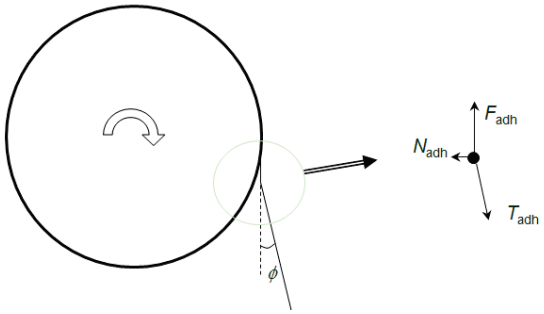

Figure 3 – The normal adhesion force component $\boldsymbol{N_{adh}}$ at a detaching web point

Remark 1. While the bending stiffness of a wet paper is usually negligible in practice, this is not the case for the fabric. However, since we are interested in millimeter-scale displacements relative to initial positions, and since the pressure gradient $\Delta p_f(x,t)$ is usually a very smooth function, we can ignore the effect bending stiffness of the fabric. For impulse pressure forces exerted in laboratory-type simulations on industrial fabrics, we have observed that the exclusion of bending stiffness usually results in a *maximum* steady-state error of approximately 5% in the deflection profile.

Remark 2. In paper machine geometries, the boundary $\mathcal{B}$ usually consists of cylinders and seals. They can be conveniently parameterized using circular arcs and line segments.

Air Flow Motion

In our FSI model, the air flow treatment is analogous to that in Immonen et al. (2009). We employ standard ANSYS Fluent control volume techniques for solving the Navier-Stokes equations for mass and momentum evolution within the air flow field (c.f. ref. [8]):

$$\frac{\partial \rho}{\partial t} + \nabla \cdot (\rho v) = 0, \quad t \geq 0 \qquad \{4a\}$$

$$\rho \frac{\partial v}{\partial t} + \rho v \cdot \nabla v = -\nabla p + \mu \nabla^2 v + f, \quad t \geq 0 \qquad \{4b\}$$

subject to geometry-specific boundary conditions and a given initial state. A flow field solution is affected by any subsequent displacements of the web and fabric; the solution {4} must thus be updated accordingly. Solution of Equations {4} yields, in particular, the pressure difference profiles $\Delta p_f(x,t)$ and $\Delta p(x,t)$ for Equations {2} and {3}.

In our simulations, air is treated as incompressible and Newtonian, with constant viscosity μ. The Navier-Stokes equations are considered in the Reynolds-averaged (RANS) sense, whereby the solution variables in the instantaneous (exact) Navier-Stokes equations are decomposed into the mean and fluctuating components. In turbulence modeling we follow the RNG $\kappa - \varepsilon$ and enhanced wall treatment approach taken, among others, by Åkerholm (2006). This two-equation turbulence model relates the ensemble-averaged velocities (Reynolds stresses) of the flow field to the kinetic energy κ and dissipation ε of turbulence. The RNG corrections and appropriate wall treatment make the methodology (at least in theory) applicable to both high and low Reynolds number flows. The approach has proven to yield fairly accurate results in the paper machine applications that we have in mind; we refer the reader to J. Åkerholm's article, ref. [7], for more details and discussion.

Cylinders and Fabric in the CFD Model

Motion of the paper web and fabric can be significantly influenced by the presence of cylinders and other equipment, which are parts of the *boundary* $\mathcal{B}$. We assume that all cylinders, if they exist in the geometry, are moving with the constant tangential velocity v which equals the axial velocity of the web and the fabric. This is usually the case in paper machine applications, although there are often slight deviations in the velocities between groups of cylinders. We ignore these deviations in the present model in order to simplify the contact treatment.

The cylinders can be reasonably treated as moving surfaces in the CFD calculations. This amounts to setting appropriate boundary conditions for Equations {4}. The fabric treatment is less trivial from the CFD point of view, however. To model fabric permeability, we follow the approach of Laakkonen (2003) and treat the fabric as a multi-layered region with resistance to air flow varying across the layers. Then the fabric's internal resistance to air flow is seen as a source term of the form:

$$f = -Dv - C|v|v \qquad \{5\}$$

in Equations {4} for the fabric's interior region. This approach has merit, because it enables one to calibrate the fabric's resistance parameters C and D to an actual industrial fabric through simulating air flows in a small three-dimensional piece of the fabric. Further details on this can be found in K. Laakkonen's thesis, see ref. [9].

Contact Treatment

The contact functions $\varkappa_f$, $\varkappa_{pf}$ and $\varkappa$ play a much more critical role in the proposed FSI model than in the model of Immonen et al. (2009). This is because there are now two deforming regions (web and fabric) instead of just one (web). Indeed, only through a careful construction of these contact functions can one be ascertained that the web and fabric cannot move through the non-deforming boundary $\mathcal{B}$, and, in particular, that the fabric cannot push the web through it. Similarly, proper contact function construction ensures that the web never penetrates the fabric in the simulations.

In the framework of the proposed FSI model, contact treatment boils down to constructing the contact functions, and then tracking contact information through the sets

$\Omega_p(t)$, $\Omega_f(t)$ and $\Omega_{pf}(t)$ during the simulations. In this subsection we describe the contact function construction and address the simulation aspect later in this article.

Remark 3. The algorithms described below depend on the contact parameters ϵ_f, ϵ_{fp} and ϵ_p. The values for these parameters cannot in our framework usually be selected independently of each other.

Fabric-boundary contact function. Let the maximum pointwise deflection $\epsilon_{defl} > 0$ be fixed. In many single-run applications a reasonable estimate is $\epsilon_{defl} = 0.03\,m$. Also fix a contact distance $\epsilon_f > 0$ (for example $\epsilon_f = 1e-4\,m$). Letting the fabric deflection $w_f(x,\cdot)$ and the corresponding point x vary, the contact function $\varkappa_f$ can be constructed via the following algorithm (recall that, by convention, $w_f(x,t) > 0$ if the fabric deforms towards the paper web at x):

1. For all $x \in [0, L]$, set $\varkappa_f\left(x, w_f(x,\cdot)\right) = 1$ whenever $\left|w_f(x,\cdot)\right| > \epsilon_{defl}$;
2. For all $x \in [0, L]$ if there is a nearby boundary point on the air-side, i.e. $d = dist\left(\mathcal{L}_{fa}(x), \mathcal{B}\right) < \epsilon_{defl}$, then set $\varkappa_f\left(x, w_f(x,\cdot)\right) = 1$ for all deflections $w_f(x,\cdot) < -d + \epsilon_f$;
3. For all $x \in [0, L]$ if there is a nearby boundary point on the web side, i.e. $d = dist\left(\mathcal{L}_{fp}(x), \mathcal{B}\right) < \epsilon_{defl}$, then set $\varkappa_f\left(x, w_f(x,\cdot)\right) = 1$ for all deflections $w_f(x,\cdot) > d - \epsilon_f$;
4. Set $\varkappa_f\left(x, w_f(x,\cdot)\right) = 0$ otherwise.

Condition 1 above restricts all deflections to be small (linear range of physics), Conditions 2 and 3 take into account fabric thickness and ensure that the fabric cannot move too close to any boundary point and Condition 4 specifies the freedom (i.e. no contact) condition.

Web-boundary contact function. The web-boundary contact function is identical to that used in Immonen et al. (2009). We restate it here for the sake of completeness. Fix a contact distance $\epsilon_p > 0$ (for example $\epsilon_p = 5e-5\,m$). Letting the deflection $w(x,\cdot)$ and the corresponding web point x vary, the contact function $\varkappa$ for the web can be constructed via the following algorithm (recall that, by convention, $w(x,t) > 0$ if the web deforms away from the fabric):

1. For all $x \in [0, L]$, set $\varkappa\left(x, w(x,\cdot)\right) = 1$ whenever $\left|w(x,\cdot)\right| > \epsilon_{defl}$;
2. For all $x \in [0, L]$ if $d = dist\left(\mathcal{L}(x), \mathcal{B}\right) < \epsilon_{defl}$, then set $\varkappa\left(x, w(x,\cdot)\right) = 1$ for all deflections $w(x,\cdot) > d - \epsilon_p$ (if d not found on the fabric side) or all deflections $w(x,\cdot) < -d + \epsilon_p$ (if d found on the fabric side);
3. Set $\varkappa\left(x, w(x,\cdot)\right) = 0$ otherwise.

Web-fabric contact function. Let the minimum admissible fabric-paper distance $\epsilon_{fp} > 0$ be given (for example $\epsilon_{fp} = 5e-5\,m$). Letting the deflections $w(x,\cdot)$ and $w_f(x,\cdot)$ and the corresponding point x vary, the web-fabric contact function $\varkappa_{fp}$ can be constructed via the following algorithm (recall that, by convention, $w(x,t) > 0$ if the web deforms away from the fabric):

1. For all $x \in [0, L]$, set $\varkappa_{pf}\left(x, w_f(x,\cdot), w(x,\cdot)\right) = 1$ whenever:

a. $w_f(x,\cdot) > w(x,\cdot) - \epsilon_{fp}$ and $w_f(x,\cdot) > 0$ and $w(x,\cdot) > 0$
b. $w(x,\cdot) < w_f(x,\cdot) + \epsilon_{fp}$ and $w_f(x,\cdot) < 0$ and $w(x,\cdot) < 0$

2. Set $\varkappa_{pf}\left(x, w_f(x,\cdot), w(x,\cdot)\right) = 0$ otherwise.

Numerical Considerations

Numerical resolution of the proposed transient FSI model is illustrated schematically in Figure 4; we use mostly the same techniques as in Immonen et al. (2009). However, in the case of a deforming fabric and deforming paper web we must pay more attention to the *order* in which calculations are carried out. The transient simulation is started at a steady-state flow field solution in which no deformations have taken place. Contact functions are also constructed using the no-deformations solution before transient simulation.

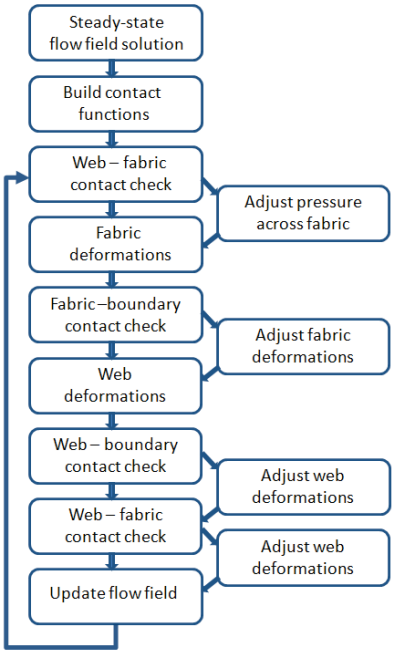

Figure 4 – Schematic representation of numerical resolution of the FSI model

By reasoning based on elementary physical principles, it is clear that fabric motion should be dominate web motion because it carries more momentum. Similarly, contact checks with respect to non-deforming boundary points should precede fabric-paper contact checks. The above schematic representation follows these principles. Furthermore, a remarkable thing to observe is that for a proper choice of ϵ_{fp}, ϵ_p and ϵ_f we can rest assured that the approach described above yields physically meaningful deformations. For example, if $\epsilon_{fp} = 5e-5\,m$, $\epsilon_p = 5e-5\,m$ and $\epsilon_f = 1e-4\,m$ the fabric cannot push the paper web through a boundary point, nor can a web point in contact with a boundary point penetrate the fabric.

APPLICATIONS TO REALISTIC SINGLE-RUN GEOMETRIES

In this section we show by two qualitative examples that the proposed FSI model yields interesting and non-trivial results for realistic single-run paper machine geometries.

Example 1

The first example involves a qualitative numerical investigation of web and fabric behavior at an opening nip region in a single-run geometry (see Figure 5). The web and fabric motion is from the top of the figure towards the bottom. The web is located between the drying cylinder and the fabric.

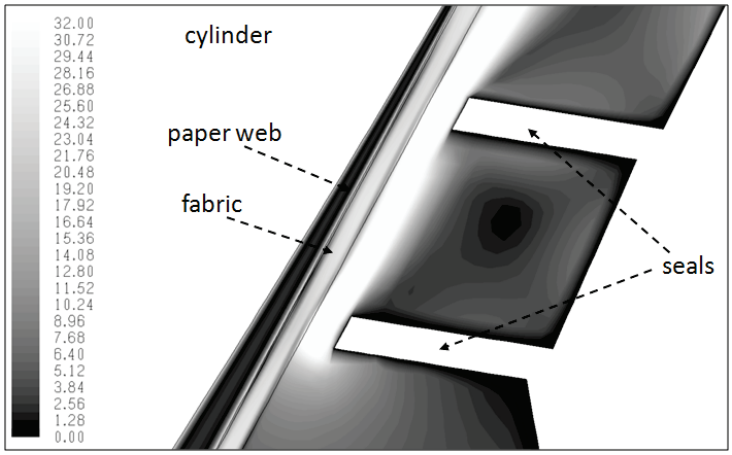

Figure 5 – Steady state velocity field (m/s) and initial web/fabric locations

It has been empirically observed that, in general, a high-velocity paper web tends to follow the drying cylinder at the opening nip due to an under-pressure effect. This effect causes runnability problems, and it can be countered by using appropriate equipment to generate a suitable pressure profile on the air side of the fabric. In the present example, there are two seals connected to an air suction device (pressure outlet in simulations) affecting the pressure profile across the web and fabric. Given the pressure outlet level, the goal was to determine if the web would still tend to follow the drying cylinder. The result of the transient simulation is depicted in Figure 6 below:

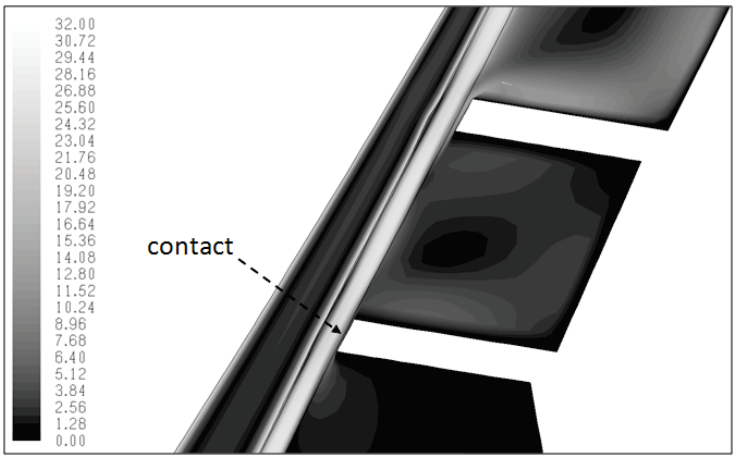

Figure 6 – Web/fabric locations and velocity field (m/s) at $t = 0.2$ seconds

Based on the simulation, we can conclude that the under-pressure generated by the suction device is in fact *too large for the present application*; the web would not tend to follow the drying cylinder, but, on the other hand, the fabric would touch the lower seal due to the large under-pressure. This would potentially damage on the fabric.

Example 2

The second example is a numerical analysis of web and fabric displacements at an open draw in a single-run geometry. The web and fabric move from the opening nip of the drying cylinder (top right) towards the closing nip of the vacuum roll (bottom left) as in Figure 7.

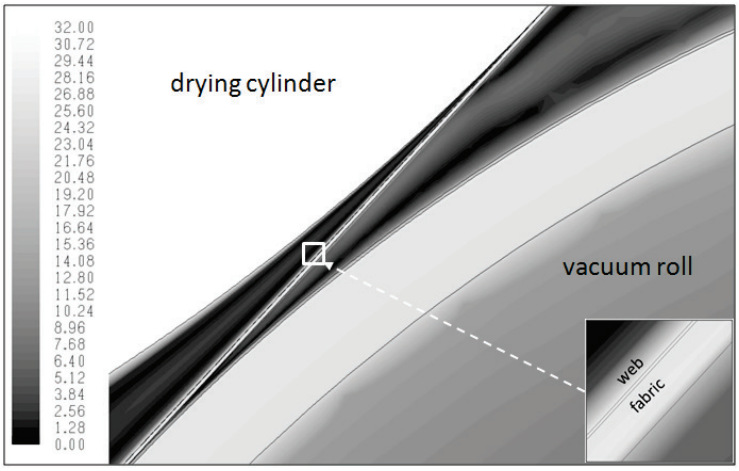

Figure 7 – Steady-state velocity profile (m/s) and initial web/fabric position

In the general case, a high-velocity paper web tends to deflect away from the fabric at the closing nip of the vacuum roll due to the over-pressure effect generated by the excess air

being carried to the closing nip in boundary layers. This effect is a source of runnability problems, but it can be countered by using e.g. a vacuum roll to remove the excess air. Given a pressure (outlet) level in the vacuum roll and the prevailing steady state pressure level in the surrounding air, we studied the transient displacement profiles of the web and fabric. In particular, the goal was to determine if the aforementioned web pocketing would take place in the given setup. The result of the transient simulation is depicted in Figure 8.

Figure 8 – Transient velocity field (m/s) and web/fabric locations at $t = 0.2$ seconds

The simulation clearly shows that undesirable web pocketing does *not* occur at the given pressure levels, and that in fact the web-fabric combination *bends significantly towards the opposite direction* at the open draw. The maximum deflection is *5-6* mm relative to the initial state. This indicates that a smaller vacuum roll outlet pressure magnitude would suffice. Notice that the FSI model also predicts the true locations of the opening nip and closing nip, which is important for appropriate positioning of runnability equipment.

CONCLUSIONS

In this article we have presented a two-dimensional FSI model for the small transverse deflections of high-velocity *paper webs and fabrics* moving in complex geometries containing non-deforming boundaries and nips. A major application of the model is single-run configured paper machines where high web velocities cause severe runnability issues (web pocketing). The proposed FSI model yields realistic and useful results for single-run setups, as was demonstrated qualitatively in the two simulated examples. A remarkable feature of the model is that it can be rapidly applied to various computational geometries thanks to the algorithmic nature of contact checks and initial curvature extraction. The main contribution of the article is to also take into account the deflections of the fabric. This is a non-trivial task due to its strictly positive thickness; only the paper web can be considered infinitely thin in applications.

Future work on the topic could concentrate on taking into account the mass and heat transfer phenomena that occur at paper machines. Another important direction for future

research is verifying the accuracy of the proposed model through measurements. At this stage, we have confined the scope of the FSI model to a conceptual level.

REFERENCES

1. Kurki, M., "Modeling of Kinematical and Rheological Web Line Behavior in a Papermaking Environment" Licenciate Thesis, Lappeenranta University of Technology, 2005.
2. Koivurova, H., "Dynamic Behaviour of an Axially Moving Membrane Interacting with the Surrounding Air and Making Contact with Supporting Structures," Doctoral Thesis, University of Oulu, 1998.
3. Karlsson, M., (Ed.), Papermaking Part 2, Drying. Fapet: Jyväskylä, 2000.
4. Chang, Y. B. and Moretti, P. M., "Edge Flutter in Webs," Proceedings of the First International Conference on Web Handling, Oklahoma, May 19-22, 1991, pp. 257-269.
5. Immonen, E., Bergström, F., Nurmi, S., Lehtinen, A., Juppi, K., and Martinsson, L., "A 2D FSI Model for Small Deflections of Fast Paper Webs Moving in Geometries Containing Nips and Boundaries," Proceedings of the Papermaking Research Symposium, Kuopio, Finland, 2009.
6. Müftü, S. and Cole, K., "Mechanics of a Cylindrical Flexible Web Floating over an Air-Reverser," Proceedings of the Fifth International Conference on Web Handling, Oklahoma, June 6-9, 1999, pp. 525-541.
7. Kurki, M. Juppi, K., Ryymin, R., Taskinen, P., and Pakarinen, P., "On the Web Tension Dynamics in an Open Draw," Proceedings of the Third International Conference on Web Handling, Oklahoma, June 18-21, 1995, pp. 230-246.
8. Åkerholm, J., "CFD Simulations in the Dry End of Paper Machines," Proceedings of the SIMS 2006, Helsinki, September 27-29, 2006.
9. Versteeg, H. and Malalasekera, W., An Introduction to Computational Fluid Dynamics - the Finite Volume Method, Prentice-Hall, 1995.
10. Laakkonen, K., "Computational Flow-Field Modeling of Paper Machine Dryer Fabric," Doctoral Thesis, Tampere University of Technology, 2003.
11. Negrut, D., Rampalli, R., Ottarsson, G., and Sajdak, A., "On an Implementation of the Hilber-Hughes-Taylor Method in the Context of Index 3 Differential-Algebraic Equations of Multibody Dynamics," J. Comput. Nonlinear Dynam., Jan 2007, 2, 1. pp. 73-85.
12. Polyanin, A. and Manzhirov, A. Handbook of Mathematics for Engineers and Scientists, Chapman & Hall, 2007.

A 2D FSI Model for Paper Webs and Fabrics Moving Close to Each Other in Complex Geometries	**E. Immonen[1], F. Bergström[1], S. Nurmi[1], A. Lehtinen[1], K. Juppi[2], & L. Martinsson[3],** [1]Process Flow Ltd Oy, [2]Metso Paper Oy, FINLAND, [3]Albany International AB, SWEDEN

Name & Affiliation	**Question**
	No Questions until Discussion